TENSILE PROPERTIES AND BENDABILITY OF B-BEARING MARTENSITIC STEELS

Jae Hoon LEE, Yeol Rae CHO, Se Don CHOO

Sheet Products & Process Research Group, POSCO Technical Research Laboratories, Jeonnam, Republic of Korea, jh-lee@posco.com

Abstract

The tensile behavior and bendability of B-bearing martensitic steels with carbon 0.15 and 0.29% were investigated. After austenitized at 900 °C for 6 min and quenched in the closed tool, full martensitic microstructure was obtained in the steels with 1.5mm in thickness. It was confirmed that the tensile strength and bending angle of the martensitic steels were significantly dependent on the carbon content; however, their bendability was independent on the elongation. It was considered that the maximum bending angle increases with increasing yield ratio. The dislocation density of martensitic steels was determined using the XRD and TEM. The peak broadening analysis of XRD profiles quantifies the dislocation density of about 1.2-2.0 × 10^{16} m^{-2}. TEM images support that 15MnB5 has a low dislocation density compared to 30MnB5. The lower number of solute carbon in 15MnB5 causes a decrease in the dislocation density during martensitic transformation. This thus results in the lower strength and higher bendability compared to 30MnB5.

Keywords: Tensile, Bendability, Dislocation Density, Martensitic Steel

1. INTRODUCTION

One of the most critical challenges for automotive industry is to reduce the weight of body in white components with a concurrent increase of safety and crashworthiness. To reduce the vehicle weight by using thinner materials with higher strength, advanced high strength steels (AHSS) are being recognized as automobile structural materials [1-3]. For an application of AHSS to complex automotive parts, inferior formability of the steels should overcome in cold forming process. Hot press forming (HPF) process has been developed currently to satisfy both high strength and good formability in manufacturing of automotive parts. There are commercially two types in the HPF manufacture method: direct and indirect process [3, 4]. The direct process is a non-isothermal forming one for sheet steels, where both forming and quenching take place in one combined process step. For example, a blank is heated at austenitization temperature, transferred to the press and then subsequently formed and quenched in the closed tool. Complete martensitic transformation in the material results in the high tensile strength [2].

X-ray diffraction (XRD) peak profile analysis is a well-established technique for the determination of microstructure in terms of dislocation density in crystalline materials [5]. Diffraction peak profiles broaden if the crystal lattice is distorted by lattice defects, especially by dislocations [6]. The size and strain effects on the diffraction peak broadening can be evaluated separately on the basis of their different *h k l* dependence [7]. For this purpose, diffraction peak patterns are evaluated by the modified William-Hall plot [8]. It is important to investigate tensile strength and bending angle of B-bearing martensitic steels, as well as their dislocation density before and after the tensile and bending tests, because the tensile properties and bendability of martensitic steels are affected by the dislocations generated by martensitic transformation and external tension. The results of the X-ray peak profile analysis will be compared to the transmission electron microscopy (TEM) observations for the B-bearing martensitic steels with different carbon content.

2. EXPERIMENTAL

Two vacuum inductions, which melted each 32 kg cast, were conducted for fabrication of B-bearing martensitic steels. The chemical composition obtained is given in **Table 1**. The slabs with 100 mm of initial thickness were heated to 1200 °C and hot-rolled to a thickness of 3 mm. The finishing temperature was kept at normal cooling one for 1 h. After cooling the strips were pickled by using hydrochloric acid and then cold-rolled to the final thickness of 1.5 mm. The cold-rolled samples were machined and used for the simulation of continuous annealing. The annealing was carried out within the intercritical temperature range, which was determined by chemical composition of the materials. A laboratory tool was used for the HPF heating and die-quenching tests, which composes symmetrically a lower and upper plate water-cooled. In order to minimize the heat loss during HPF process, the specimens are placed on the pins which disappear in the die when a pressure is applied. The cold-rolled, annealed sheets were heated at 900 °C for 6 m for a homogeneous austenitization of the microstructure.

Table 1 Chemical composition of materials used here (wt.%)

Material	C	Si	Mn	P	S	Al	Cr	Ti	B	N
15MnB5	0.15	0.25	1.29	0.01	0.003	0.025	0.16	0.029	0.0019	0.0036
30MnB5	0.29	0.26	1.25	0.01	0.003	0.029	0.16	0.029	0.0019	0.0026

The microstructure of the HPF-heated + die-quenched samples were observed by optical microscopy (OM) and TEM. The disc-type specimens (3 mm in diameter) were prepared by mechanical polishing followed by twin-jet electro-polishing in a solution of 10 vol.% $HClO_4$ + 90 vol.% CH_3COOH (acetic acid) at 15°C at a voltage of 20 V. The high-resolution X-ray diffractometer was used with a copper (Cu $K_{\alpha 1}$) radiation (wavelength, λ = 0.15406 nm). The scattered radiation covered about 2θ = 40-110° of the angular range of diffractions.

Transverse plane sections of the martensitic steels HPF-heated and die-quenched were prepared for tensile and 3-point bending tests. The specimens were taken in transverse direction and machined to JIS No.5 (width: 25 mm, gauge length: 50 mm) for tensile tests and 20 x 60 x 1.5 mm^3 for bending tests, respectively. For the two samples, the average value of three specimens was measured to calculate the yield strength, tensile strength, total elongation and bending angle at maximum force (α at F_{max}). The tensile and 3-point bending tests were carried out under the stroke control mode with the crosshead speed of 10 mm/m and 20 mm/m, respectively. Note that a bending punch had to be designed such that, while testing, the samples had contact with the punch radius only. The samples were positioned symmetrically on both rollers such that the force applied via the bending punch acted along the center of the distance between the supports. The punch radius (R) used in these experiments was 0.4 mm [9].

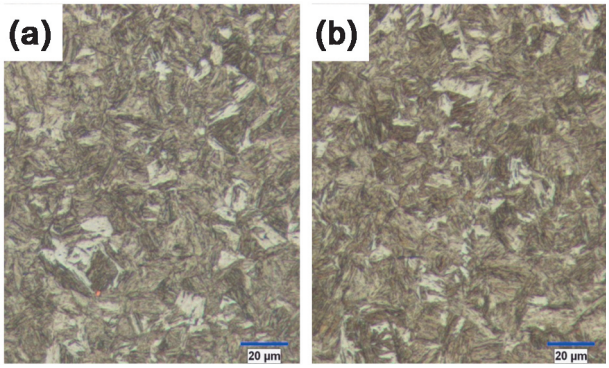

Fig. 1 Microstructure of (a) die-quenched 15MnB5 and (b) 30MnB5

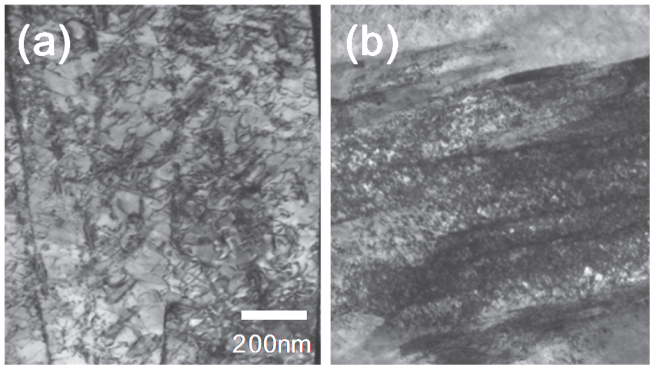

Fig. 2 TEM micrographs of die-quenched 15MnB5 and (b) 30MnB5

3. RESULTS AND DISCUSSION

3.1 Microstructure analysis

Fig. 1 shows that the microstructure of the martensitic steels with carbon of 0.15 and 0.29%. It is confirmed that the increasing carbon content reduces the size of lath martensite. Two TEM bright-field images are shown in **Fig. 2**. The images show the dislocation-embedded lath structure in the 15MnB5 sample (**Fig. 2-a**) and the 30MnB5 one (**Fig. 2-b**). It is evident that the B-bearing steel with higher carbon content contains a larger number of dislocations (black line segments) compared to the 15MnB5 that possesses the smaller number of solute carbon in the steel matrix, which doesn't diffuse into the matrix during fast die-quenching. The smaller size of lath martensite of 30MnB5 is considered to be due to more of dislocations than 15MnB5's ones.

3.2 Tensile and bending properties

Fig. 3 shows the tensile behaviors of the die-quenched martensitic steels. The strength of martensitic steels is strongly dependent on the carbon content; but the steels have relatively weak dependence on the elongation. It is interesting to note that the result of a lower yield ratio (YS/TS) of 30MnB5 than 15MnB5 is likely influenced by the number of solute carbon.

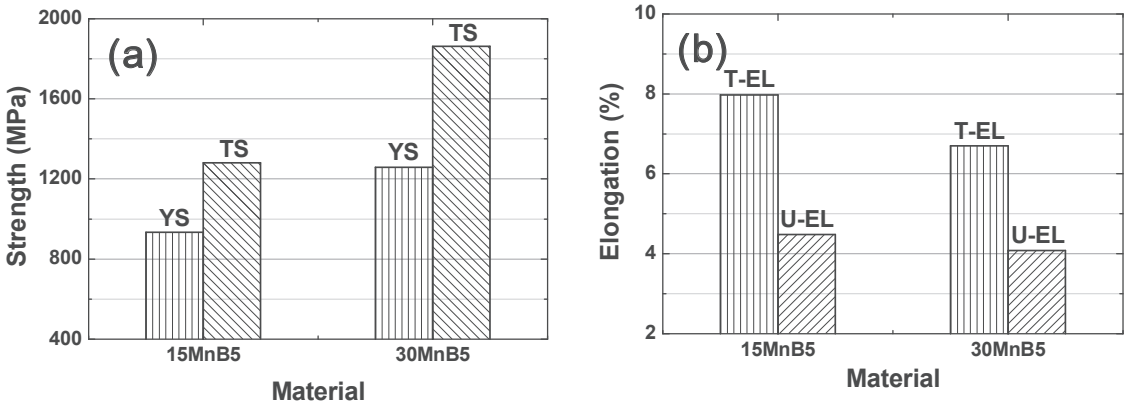

Fig. 3 Strength (a) and elongation (b) of die-quenched 15MnB5 and 30MnB5

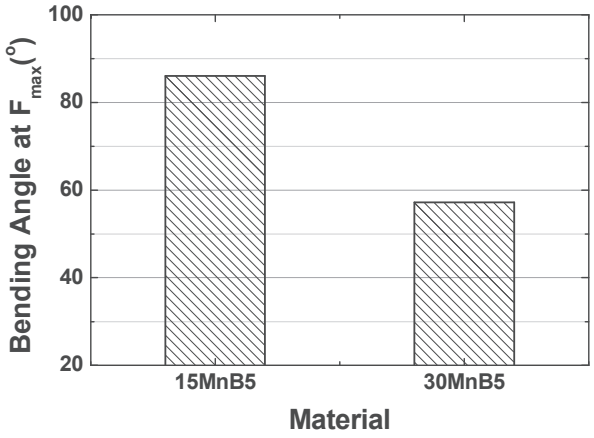

Fig. 4 Bending angle at maximum force of die-quenched 15MnB5 and 30MnB5

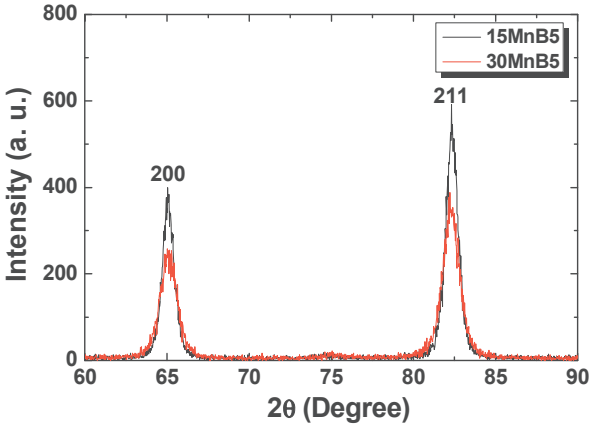

Fig. 5 XRD peaks of die-quenched 15MnB5 and 30MnB5 correspond to (200) and (211) diffraction peaks, respectively

It is known that surface strains of sheet steels are caused during bending, which are much larger than those induced during tensile test. The bendability is expressed as bending angle at maximum force during the 3-point bending test. The maximum bending angle of both 15MnB5 and 30MnB5 is represented in **Fig. 4**. The bending angle of B-bearing martensitic steels significantly decreases with the increase of carbon content. Note that the bendability of martensitic steels is influenced by the bending-induced work hardening which is relevant to the increasing solute carbons in martensitic matrix. It was reported that in comparison to ferritic steels, the bending behaviors of martensitic steels are accelerated significantly by the bending-induced work hardening possessing the strong carbon dependence, although both materials have same alloying compositions [10].

3.3 Dislocation density

Fig. 5 shows the example of the directly measured X-ray diffractogram at 1.1mm location of the cross-section of the 15MnB5 and 30MnB5 materials. The (200) and (211) reflection profiles show that the peak broadening of 30MnB5 is larger than that of 15MnB5. Such difference in the peak broadening is likely related to the different dislocation densities produced by martensitic transformation.

The Williamson-Hall plot shows the qualitative behavior of diffraction peak broadening with the full width at half maximum (FWHM) as a function of K, where $K = 2 \sin \theta/\lambda$, θ and λ are the diffraction angle and the wavelength of the X-ray, respectively [8]. Strain anisotropy in the conventional Williamson-Hall plot has been rationalized as replacing K by $KC^{1/2}$ in the modified Williamson-Hall plot [8]. Note that the C is the dislocation contrast factor, which can be determined by the elastic anisotropy and the dislocation type of materials [7]. The FWHM are plotted as $\Delta K = 2 \cos \theta(\Delta\theta)/\lambda$ in 1/nm scale, where $\Delta\theta$ is the FWHM obtained from each (hkl) peak as shown in **Fig. 5**.

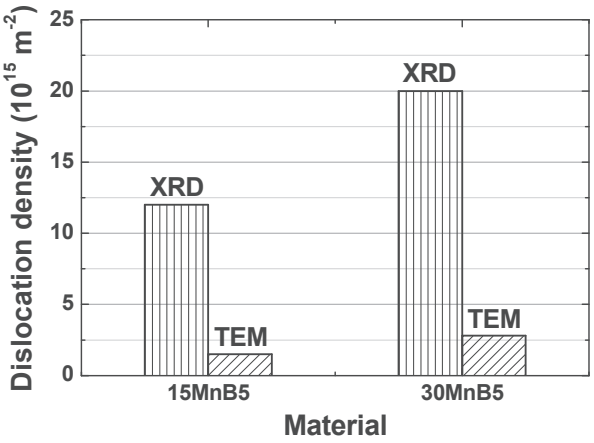

Fig. 6 Dislocation densities of die-quenched 15MnB5 and 30MnB5 evaluated by the XRD and TEM method

As aforementioned, the tensile properties and bendability of martensitic steels are affected by the dislocation density that is closely related to the straining due to the martensitic transformation and external tension. This study focused on the dislocation density induced by the martensitic transformation. Note that we are keeping up the study of dislocations induced by the external tension and the analysis of a relationship between the dislocation density and strain hardening behavior for the martensitic steels. **Fig. 6** shows the dislocation density of die-quenched martensitic steels evaluated by the XRD method and TEM observation. The dislocation density (2.0×10^{16} m^{-2}) of 30MnB5 analyzed by XRD is larger than that of 15MnB5 (1.2×10^{16} m^{-2}), indicating the dependence on the number of solute carbon. Interestingly, the XRD method gives a difference higher by nearly an order of magnitude as compared with the TEM analysis. The lower dislocation density analyzed by TEM is likely explained by the inhomogeneous distribution of dislocations in martensitic steels. This is consistent with other quantitative TEM observations reported by Morito, Kehoe, and Nostrom [11-13].

CONCLUSIONS

The tensile properties and bendability of B-bearing martensitic steels with carbon of 0.15 and 0.29% were examined. After HPF heating and die-quenching the total elongation of martensitic steels scarcely depends on the increasing carbon content. The bendability of die-quenched steels has significantly relevance to the yield ratio, where the maximum bending angle increases with increasing yield ratio. The dislocation density of martensitic steels was determined using the XRD and TEM. The peak broadening analysis of XRD profiles quantifies the dislocation density of about 1.2-2.0 × 10^{16} m^{-2}. TEM images support that 15MnB5 has a low dislocation density compared to 30MnB5. The lower number of solute carbon in 15MnB5 causes a decrease in the dislocation density during martensitic transformation. This thus results in the lower strength and higher bendability compared to 30MnB5.

ACKNOWLEDGEMENTS

The authors acknowledge the many helpful discussions with Dr. LEE G.Y. and KIM S.G. of POSCO Technical Research Laboratories.

REFERENCES

[1] PAAR U., BECKER H.H., ALSMANN M. Press-hardened components from Kassel-chances and challenges, In Proc. *the 1st Hot Sheet Metal Forming of High-Performance Steel*, CHS2, Kassel, 2008, 153-164.

[2] STEINHOFF K., SCHUPFER M., ADEMAJ A., WEIDIG U. All about Press Hardening - An Overview on Technology and Markets, In Proc. *the 2nd International Seminar on Hot Sheet Metal Forming of High-Performance Steel*, CHS2, Hanover, 2012, 64-89.

[3] KARBASIAN H., TEKKAYA A.E. A review of hot stamping, *Journal of Materials Processing Technology*, 210, 2010, 2103-2118.

[4] FAN D.W., KIM H.S., DeCooman B.C. A review of the physical metallurgy related to the hot press forming of advanced high strength steel, *Steel Research International*, 80, 2009, 241-248.

[5] KRIVOGLAZ M.A. *Theory of X-ray and Thermal Neutron Scattering by Real Crystals*, Plenum Press, New York, 1996.

[6] CULLITY B.D., STOCK S.R. *Elements of X-ray Diffraction*, Prentice Hall, Upper Saddle River, 2001.

[7] UNGAR T., DRAGOMIR I., REVESZ A., BORBELY A. The contrast factors of dislocations in cubic crystals: the dislocation model of strain anisotropy in practice, *Journal of Applied Crystallography*, 32, 1999, 992-1002.

[8] UNGAR T., BORBELY A. The effect of dislocation contrast an x-ray line broadening: A new approach to line profile analysis, *Applied Physics Letters*, 69, 1996, 3173-3175.

[9] BMW Gr. *Bending test for evaluating crash behavior of high-strength steels*, AA-M 246, 2009, 1-4.

[10] LEE J.H., CHO Y.R., CHOO S.D. Investigation of Tensile Properties and Bendability of CMnB Hot-Press Forming Steels, In Proc. *the 4th Hot Sheet Metal Forming of High-Performance Steel*, CHS2, Luleå, 2013, 217-226.

[11] MORITO S., NISHIKAWA J., MAKI T. Dislocation density within lath martensite in Fe-C and Fe-Ni alloys, *ISIJ International*, 43, 2003, 1475-1477.

[12] KEHOE M., KELLY P.M. The role of carbon in the strength of ferrous martensite, *Scripta Metallurgica*, 4, 1970, 473-476.

[13] NOSTROM L.A. On the Yield Strength of Quenched Low-Carbon Lath Martensite, *Scandinavian Journal of Metallurgy*, 5, 1976, 159-165.